ISSN 0543-5846
METABK 55(2) 225-228 (2016)
UDC – UDK 621.791.052:621.72:536.5:620.18=111

THE MODELING OF HEAT AFFECTED ZONE (HAZ) IN SUBMERGED ARC WELDING (SAW) SURFACING STEEL ELEMENT

Received – Primljeno: 2015-03-06
Accepted – Prihvaćeno: 2015-09-15
Preliminary Note – Prethodno priopćenje

In the work the bimodal heat source model in the description of the temperature field is presented. The electric arc was treated physically as one heat source, whose heat was divided: part of the heat is transferred by the direct impact of the electric arc, but another part of the heat is transferred to the weld by the melted material of the electrode. Computations of the temperature field during SAW surfacing of S355 steel element are carried out. The macrographic and metallographic analysis of the weld confirmed the depth and shapes of the fusion line and HAZ defined by the numerical simulation.

Key words: SAW, HAZ, modeling, temperature, microstructure

INTRODUCTION

In the modelling of the temperature field of welding processes a single-distributed heat source model is generally assumed, reflecting the direct impact of the electric arc on the surfaced object. This approach is found in the description of the temperature field during SAW surfacing using analytical and numerical methods [1-4]. The shape of the fusion lines during surfacing by welding often exhibit shape irregularity that is difficult to restore by means of the description of the temperature field obtained by using the single-distributed heat source model.

MODEL OF TEMPERATURE FIELD

The part of the heat generated by the electric arc is consumed to heat and melt the electrode or the additional material, and then transferred by the cooling weld material to the surfaced object. This gives a justification for the division of the heat generated by an electric arc. The proposed model assumes physically one heat source – an electric arc, and the heat transfer to the surfaced object is divided into the heat transferred directly through the electric arc and through molten material in the form of drops, that under the influence of electromagnetic forces are detached and transferred to the forming weld. The proposed solution of the temperature field is summing temperature fields caused by the heat of direct impact of an electric arc and the heat transferred to the surfaced object through the molten electrode material. It was assumed that the volume of the weld reinforcement and the heat accumulated there are approximately equal to the volume of molten electrode wire and the amount of the heat consumed for melting the electrode. This allows the formulation of the temperature field in the form:

$$T\,(x, y, z, t) - T_0 = T_a\,(x, y, z, t) + T_w(x, y, z, t) \quad (1)$$

where: $T_a(x,y,z,t)$ and $T_w(x,y,z,t)$ are tempera-ture fields caused respectively by the heat of direct impact of an electric arc and by the heat of the weld reinforcement (consumed to melt the electrode).

The shape of the weld face is determined mainly by the forces of surface tension. On the basis of experimental research Hrabe and others [5] have proposed a parabolic shape of the face. Lower limit of the imposed metal is defined by the surface shape of surfaced material. In the solution the parabolic model was adopted. Then the geometry of the weld is presented in Figure 1, where h_w is the height of the weld (weld reinforcement – the part of the weld above the surface of the surfaced material), d_p is the depth of material thickness loss (e.g. depth of wear zone), and Δl results from considering the volume of material supplied from the electrode.

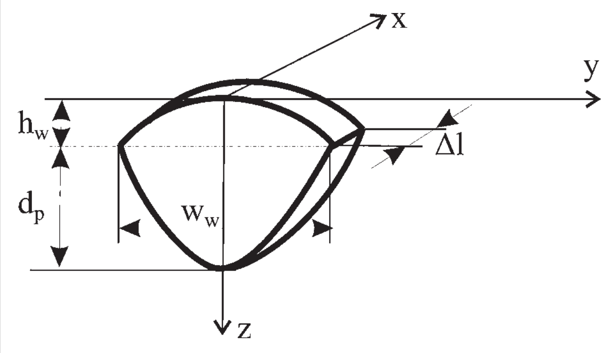

Figure 1 Geometry of the weld

J. Winczek, E. Gawrońska, Faculty Mech. Eng. and Comp. Science, Czestochowa University of Technology, Poland

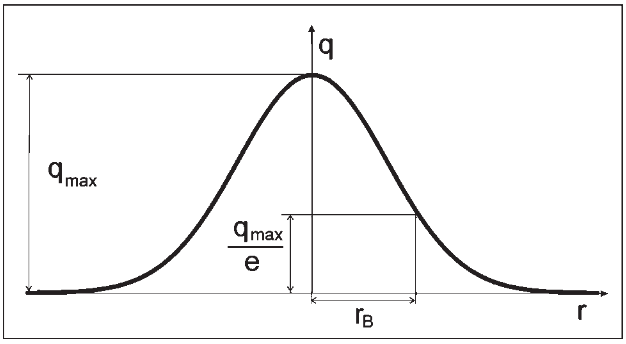

Figure 2 Gaussian distribution of heat source

Analytical description of the temperature field caused by the direct impact of the electric arc with Gaussian heat distribution (Figure 2) is shown in [6], whereas considering the heat stored in the liquid metal imposed on the surface is presented in [7].

For accepted scheme of the single-pass surfacing (Figure 3), where: $\xi = x - vt - x_0$ and x_0 is the coordinate of the start of the weld, the temperature field (1) is defined as follows:

- for time $t > t_c$, where t_c is the total time of making of the weld:

$$T(x,y,z,z_0,t) - T_0 = \\ = A_w \int_0^t \{H_H(t'')(F_2(y,z) + F_3(y,z) - F_4(y,z) + \\ - F_1(y,z))\}dt'' + A_H \int_0^t F_H(t'')dt'' \quad (2)$$

- for time $t > t_c$:

$$T(x,y,z,z_0,t) - T_0 = \\ = A_w \int_0^{t_c} \{H_C(t')(G_2(y,z) + G_3(y,z) - G_4(y,z) + \\ - G_1(y,z))\} + A_C \int_0^{t_c} F_C(t')dt' \quad (3)$$

where

$$t_c = l / v \quad (4)$$

$$A_H = \frac{3\dot{q}}{16C_p\rho(\pi a)^{1,5} z_0} \exp\left(-\frac{\xi v}{2a} - \frac{v^2 t_0}{4a}\right) \quad (5)$$

$$A_C = 3\dot{q} / (16C_p \rho \pi a z_0) \quad (6)$$

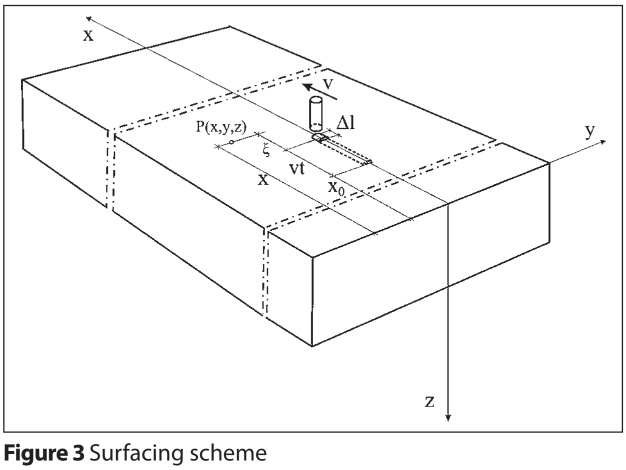

Figure 3 Surfacing scheme

$$A_w = \dot{q}_v / 8c\rho\sqrt{\pi a} \quad (7)$$

$$F_H(t'') = \frac{1}{t''+t_0} \exp\left(-\frac{\xi^2}{4a(t''+t_0)} - \frac{v^2 t''}{4a}\right) \\ \left\{\left(1 - \frac{z^2 + 2at''}{z_0^2}\right)\left(\left(erf\left(\frac{z+z_0}{2(at'')^{0,5}}\right.\right.\right. \\ \left.\left. - \Phi(z) erf\left(\Phi(z)(z)\frac{z-z_0}{2(at'')^{0,5}}\right)\right)\right) + \\ \frac{4at''}{z_0^2}\left(\frac{z+z_0}{(4\pi at'')^{0,5}}\exp\left(-\frac{(z-z_0)^2}{4at''}\right)\right. \\ \left.\left. - \frac{z-z_0}{(4\pi at'')^{0,5}}\exp\left(-\frac{(z+z_0)^2}{4at''}\right)\right)\right\} \quad (8)$$

$$H_H(t'') = \frac{1}{\sqrt{t''}}\left(erf\left(\frac{\Delta l - 2(\xi + vt'')}{4\sqrt{at''}}\right) + \right. \\ \left. + erf\left(\frac{\Delta l + 2(\xi + vt'')}{4\sqrt{at''}}\right)\right) \quad (9)$$

$$\Phi(z) = \begin{cases} -1 & dla \quad z \in <0, z_0> \\ 1 & dla \quad z \in (z_0, \infty) \end{cases} \quad (10)$$

$$F_C(t') = \frac{1}{t + t_0 - t'} \\ \exp\left(-\frac{(x - v\,t' - x_0)^2 + (y - y_0)^2}{4a(t + t_0 - t')}\right) \\ \left\{\left(1 - \frac{z^2 + 2a(t-t')}{z_0^2}\right)\left(erf\left(\frac{z+z_0}{2(a(t-t'))^{0,5}}\right)\right.\right. \\ \left. - \Phi(z) erf\left(\Phi(z)\frac{z-z_0}{2(a(t-t'))^{0,5}}\right)\right) + \\ \frac{4a(t-t')}{z_0^2}\left(\frac{z+z_0}{(4\pi a(t-t'))^{0,5}}\exp\left(-\frac{(z-z_0)^2}{4a(t-t')}\right)\right. \\ \left.\left. - \frac{z-z_0}{(4\pi a(t-t'))^{0,5}}\exp\left(-\frac{(z+z_0)^2}{4a(t-t')}\right)\right)\right\} \quad (11)$$

$$H_C(t') = \frac{1}{\sqrt{(t-t')}}\left(erf\left(\frac{\Delta l - 2(x - vt' - x_0)}{4\sqrt{a(t-t')}}\right) + \right. \\ \left. + erf\left(\frac{\Delta l + 2(x - vt' - x_0)}{4\sqrt{a(t-t')}}\right)\right) \quad (12)$$

a - thermal diffusivity / $m^2 s^{-1}$, C_p - specific heat / J $kg^{-1} K^{-1}$, ρ - density / kg m^{-3}, x_0 / m and l / m are the coordinates of the start and length of the weld respectively. Quantity t_0 / s characterizes surface heat source distribution whereas $r_B^2 = 4at_0$ [8] (compare Figure 2). Functions $G_1 - G_4$ and $F_1 - F_4$ are solutions of integrals using Gauss-Legendre quadrature [7].

The total amount of the heat q_v contained in the material of melted electrode is presented by formula [9]:

$$q_v = \Delta q_{solid} + \Delta q_f + \Delta q_{liqiud} \tag{13}$$

where Δq_{solid} – the heat required to heat the electrode from the initial temperature to the melting point, Δq_f – the heat used to melt the electrode (heat of fusion), Δq_{liquid} – the heat used to heat melted material to the temperature, where a drop of metal falls onto the surface of the surfaced object.

The initial value of the outputted from the welding head electrode temperature is determined on the 100 °C. Accordingly:

$$\dot{q}_v = \dot{m}\left(c\left(T_L - T_e\right) + L\right) \tag{14}$$

where L is the heat of solidification /J kg^{-1},

$$\dot{m} = \rho_e \frac{\pi d^2}{4} v_e \tag{15}$$

where: d is the diameter of the electrode, ρ_e is the density of the electrode material and v_e is wire feed speed.

EXAMPLE OF CALCULATION

Calculations of the changeable in time temperature field for a square steel element with the side length 0,2 m and thickness of the plate 0,03 m made from steels S355J2G3 have been conducted. Thermal properties of welded subject material and electrode have been determined by $a = 8 \cdot 10^{-6}$ m^{2}s^{-1}, C_p = 670 J kg^{-1} K^{-1}, ρ = 7 800 kg m^{-3} and L = 268 kJ kg^{-1}.

Numerical simulation has been conducted for the welding heat source of power 3 500 W with Gaussian power density distribution determined by t_0 = 0,13 s and z_0 = 0,008 m.

The source power corresponds to welding parameters (U = 30 V, I = 400 A, η = 0,95) used in the welding experiment. Likewise in the experiment in calculations there were assumed welding velocity v = 0,007 m s^{-1}, electrode wire diameter d = 3,5 mm, wire feed speed v_e = 0,031 m s^{-1} and bead dimensions h_w = 2,5 mm and w_w = 22 mm (d_p = 0). The initial value of temperature of electrode T_e = 100 °C (a temperature of contact tip with the welding head). Computations have been made for middle cross-section of the surfaced element.

In Figure 4 maximum temperature distribution in cross section has been presented. The calculted isotherm 1 493 °C determines the fusion line and isotherms A_3 and A_1 determine the partial and full austenitization zones (Figure 5). The temperatures A_3 = 920 °C and A_1 = 748 °C have been calculated taking into account the effect of heating rate on the temperature [10, 11].

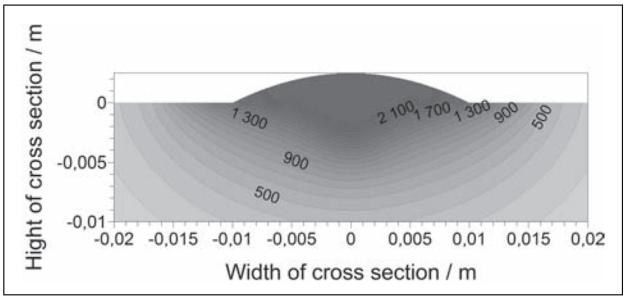

Figure 4 Maximum temperature field

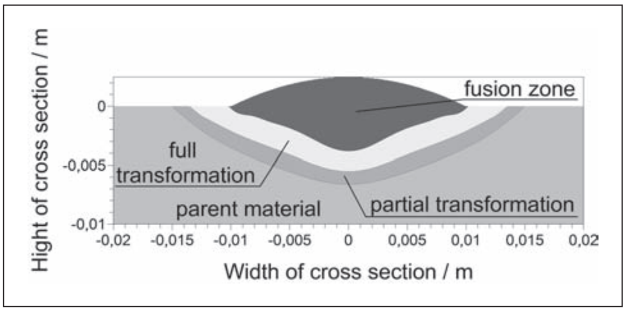

Figure 5 Calculated heat affected zones.

EXPERIMENTAL WORK

The attempts were made at submerged arc surfacing of a square plate measuring 200 mm x 200 mm and thickness of 30 mm, made of steel S355J2G3, with the following parameters: U = 30 V, I = 400 A and v = 0,5 m min^{-1}. The photograph of a metallographic macrosection in the middle cross section is shown in Figure 6. Dimensions of the weld: height of the weld reinforcement – 2,5 mm, width of the weld – 18 mm, depth of fusion in the weld axis – 3,4 mm. Calculated solidus isotherm 1 493 °C (solidification temperature of steel) - black line - corresponds to the fusion line obtained in an experiment. Bright line corresponds to the calculated temperature limit of the full transformation of austenite A_3.

The metallographic analysis is performed confirming the identification of the highlighted areas: fusion and the full austenite transformation zones. Results are compared with the structure of the parent material. In the reinforcement of the weld and in the fusion zone (Figure 7) there is visible dendritic, ferriticpearlitic structure with Widmanstätten structure near the fusion line (Figure 8). The heat affected zone (Figure 9) is characterized by fine-grained, ferritic-pearlitic structure. The parent material structure is presented in Figure 10.

CONCLUSIONS

Taking into account the heat of the molten metal in the descriptions of the temperature field in the surfacing processes allows the reproduction of the shapes and dimensions of the fusion lines formed in surfacing prac-

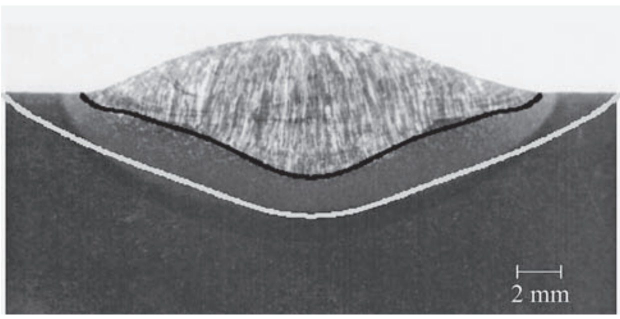

Figure 6 Comparison of numerical results and image of metallographic section

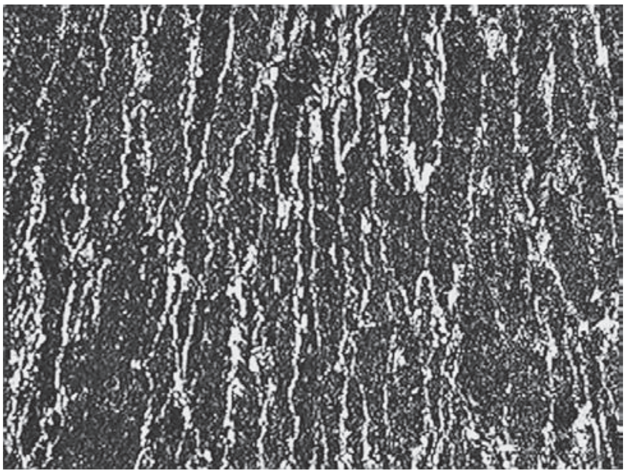

Figure 7 Weld, Nital Etch, 100x, pearlitic-ferritic, dendritic structure

Figure 8 Weld near fuison line, Nital Etch, 100x, pearlitic-ferritic, Widmanstätten structure

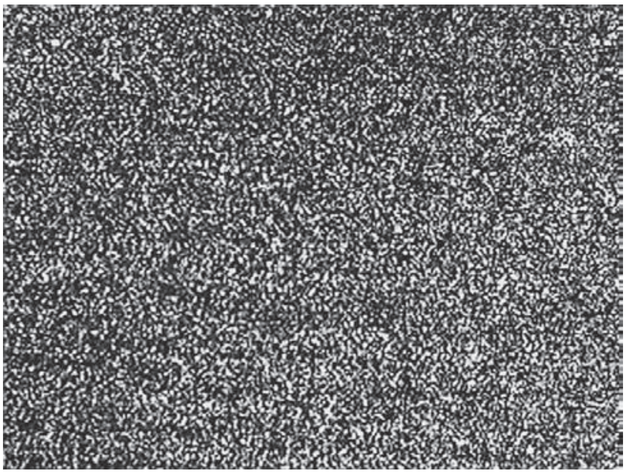

Figure 9 Heat affected zone, Nital Etch, 100x, fine-grained, ferritic-pearlitic structure

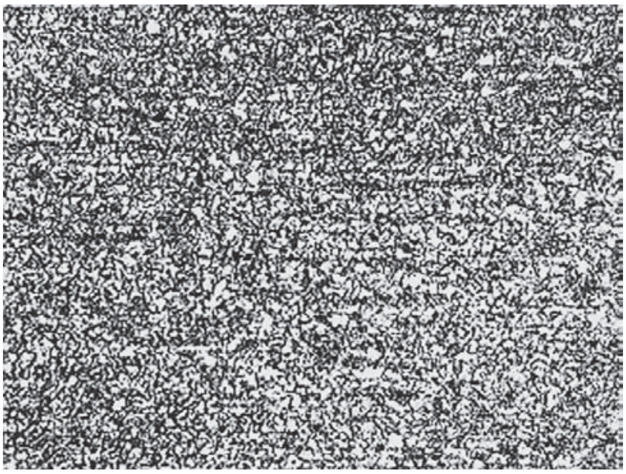

Figure 10Parent material, Nital Etch, 100x, ferritic-pearlitic structure

tice. The macrographic inspections of the weld confirm the depth and regular shapes of the heat affected zone defined by the numerical simulation. The metallographic analysis shows the material structure characteristic for the identified zones (dendritic structure in the reinforcement of the weld and the fusion zone, fine grain structure in fully austenitic transformation). The direction for further research is to analyze the correlation between the parameters of the heat source model and technological parameters of the process and their impact on the temperature distribution (dimensions and shapes of the fusion lines and also the heat affected zones) as well as the kinetics of phase transformation.

REFERENCES

[1] R. Parkitny, A. Pawlak, W. Piekarska, Thermal model of submerged arc welding process, Mat. Sci. Tech. 8 (1992), 841-843

[2] V. Gunaraj, N. Murugan, Prediction of heat-affected zone characteristics in submerged arc welding of structural steel pipes, Weld. J. 81 (2002), 94s-98s

[3] A. K. Pathak, G. L. Datta, Three-dimensional finite element analysis to predict the different zones of microstructure in submerged arc welding, Proc. Inst. Mech. Eng. B, 218 (2004), 269-280

[4] A. Ghosh, N. Barman, H. Chattopadhyay, S. Hloch, A study of thermal behaviour during submerged arc welding, Strojniški vestnik – J. Mech. Eng. 59 (2013) 5, 333-338

[5] P. Hrabe, R. Choteborsky, M. Navratilova, Influence of welding parameters on geometry of weld deposit bead, Proceedings, Int. Conf. on Economic Engineering and Manufacturing Systems, Brasov, 2009, Regent 10, 27, pp. 291-294

[6] J. Winczek, Analytical solution to transient temperature field in a half-infinite body caused by moving volumetric heat source, Int. J. Heat Mass Transfer 53 (2010), 5774-5781

[7] J. Winczek, New approach to modeling of temperature field in surfaced steel elements, Int. J. Heat Mass Transfer, 54 (2011) 4702-4709

[8] P. R. Vishnu, W. B. Li, K. E. Easterling, Heat-flow model for pulsed welding, Mat. Sci. Tech. 7 (1991), 649-659

[9] P. J. Modenesi; R. I. Reis, A model for melting rate phenomena in GMA welding, J. Mater. Proccess. Tech. 189 (2007), 199-205

[10] W. Piekarska, M. Kubiak, Z. Saternus, Numerical simulation of thermal phenomena and phase transformations in laser-arc hybrid welded joints, Arch. Metall. Mater. 56 (2011), 409-421

[11] J. W. Elmer, T. A. Palmer, W. Zhang, B. Wood, T. DebRoy, Kinetic modeling of phase transformations occurring in the HAZ of C-Mn welds based on direct observations, Acta Mater. 51 (2003), 3333-3349

Note: The responsible translator for English language is Izabela Mishchil, Częstochowa, Poland